Journal of Alloys and Compounds 480 (2009) 741–746

Contents lists available at ScienceDirect

Journal of Alloys and Compounds

journal homepage: www.elsevier.com/locate/jallcom

Oriented ZnO nanoplates on Al substrate by solution growth technique

J.P. Cheng*, Z.M. Liao, D. Shi, F. Liu, X.B. Zhang

Department of Materials Science and Engineering, State Key Laboratory of Silicon Materials, Zhejiang University, Hangzhou 310027, China

ARTICLE INFO

Article history:
Received 7 December 2008
Received in revised form 8 February 2009
Accepted 10 February 2009
Available online 23 February 2009

Keywords:
Oxide materials
Thin films
Chemical synthesis
Optical properties
Scanning electron microscopy

ABSTRACT

ZnO nanoplate thin films have been synthesized by a one-step solution technique in a surfactant-free system. The structure and morphology of the fabricated ZnO nanoplates were characterized by X-ray diffraction, scanning electron microscopy and transmission electron microscopy. These network-like nanoplates were dispersed quasi-vertically and homogenously on aluminum substrates. The size of ZnO nanoplate was depended on the reaction temperature. Increasing the reaction temperature would result in much thicker and wider ZnO nanoplates. The density of ZnO nanoplates was determined by zinc concentration. Under high temperature, these ZnO nanoplates tended to recrystallization and its density would decrease. Photoluminescence properties of the as-prepared and annealed ZnO nanoplate films were studied in this work.

1. Introduction

Oriented growth of nanostructured inorganic solid on conductive substrates possesses prospective significance in manufacturing electronic and optoelectrinic nanodevices [1–3], especially for semi-conductor materials, such as ZnO, SnO_2, TiO_2, etc., having enormous potential as building blocks for electronic, photonic, and sensor devices. Especially, for the past few years, a wide variety of ZnO nanostructures have been prepared, including rods, wires, belts, tubes, cages, walls, spirals, rings, flowers, and so on [2–5]. However, for the nanostructured ZnO building blocks to incorporate into nanodevices, the control of the synthesized nanostructures for desired size, shape, and orientation should be first fulfilled and this is a rather challenging issue [2,5,6]. Substantial efforts had been devoted to the synthesis of uniform shape-controlled ZnO nanostructures on conductive substrates [2,5–9].

Two-dimensional (2D) nano-scaled sheets or platelets of ZnO with a high surface to volume ratio are suggested to be ideal objects for the nanodevices used in energy storage and conversion [10], chemical and biological sensors, solar cells, field emission [7–9,11] and photocatalytic degradation of organic dye [12]. However, studies regarding 2D ZnO nanostructures are less common compared those regarding 1D ZnO nanomaterials. Ryan and co-workers reported an electrochemical method to grow vertically ZnO nanoplates on Zn foil, where small variations in the electrochemical potential gave rise to a variety of crystal morphologies including 1D and 3D growth [13]. Fujihuara and co-workers fabricated oriented ZnO nanoplates on glass slide with layered hydroxide zinc acetate as precursor by pyrolytic transformation [14]. Su and co-workers reported a hydrothermal procedure for high-yield synthesis of ZnO hexagonal nanoplates on Zn foil [15]. Ye et al. reported ZnO nanoplates as thin as 10 nm on Al substrate that had higher efficiency in photodegrading organic dyes than ZnO nanorods did [12]. Recently, Weng and co-workers applied a two-step route to prepare ZnO nanosheets on Si substrate on which ZnO seed-layer was pre-coated [16]. Quasi-vertical ZnO nanosheet films had been synthesized by solvothermal route on copper substrates and their field emission properties had also been investigated by Bai et al. [8].

There have a strong demand for low-cost and simple fabrication on 2D ZnO synthesis. In contrast to energy-consuming vapor phase method [4,5], the solution method can be carried out in soft environments on a large scale. Hence, it is worth investigating to realize the controllable synthesis of ZnO nanoplates with good orientation on conductive substrates through chemical solution method. In this work, ZnO network-like nanoplate films with orientation are prepared through a simple solution technique on metallic Al substrate. The variation in reaction conditions is discussed in detail. Our results represent a cost effective method on the fabrication of metal-oxide nanostructures for large scale applications.

2. Experimental

The procedure to prepare ZnO nanoplate films was simplified from our previous method [17], similarly to what Ye et al. reported [12]. A high-purity aluminum slice as substrate, rinsed with acetone and deionized water in the ultrasonic cleaner, was immersed into the reaction solution under mild temperature.

---

* Corresponding author. Tel.: +86 571 87951411; fax: +86 571 87951411.
E-mail address: chengjp@zju.edu.cn (J.P. Cheng).

0925-8388/$ – see front matter © 2009 Elsevier B.V. All rights reserved.
doi:10.1016/j.jallcom.2009.02.041

Table 1
Summarized experimental conditions on the synthesis of ZnO nanoplate films.

Sample code	Zn^{2+} con. (M)	HMT con. (M)	Growth temp. (°C)	Annealing temp. (°C)
S1	0.02	0.02	90	
S2	0.02	0.02	120	
S3	0.02	0.02	150	
S4	0.2	0.02	120	
S5	0.2	0.2	120	
S6	0.02	0.2	120	
S7	0.02	0.2	120	500
S8	0.2	0.02	120	500

In a typical experiment, the reaction solution was composed of equal volume of zinc nitrate ($Zn(NO_3)_2$) solution with concentrations from 0.02 to 0.2 M and hexamethylenetetramine (HMT) solution with concentrations from 0.02 to 0.2 M. All of the solutions were prepared with reagent-grade chemicals and deionized water. The mixture solution was transferred into a Teflon-lined stainless steel autoclave and an Al substrate was vertically dipped into the nutrient solution. The autoclave was sealed and heated to a constant temperature from 90 to 150 °C for 2 h. After cooling to room temperature naturally, a white layer of product was covered on the Al substrate. The resulted thin film was thoroughly washed with deionized water and ethanol, respectively, to eliminate residual salts, and dried in air at 50 °C for hours. For comparison, parallel experiments were also carried out under various conditions that were listed in Table 1. The obtained product was denoted as different code. In annealing process, Al substrates covered with ZnO films were subjected to thermal annealing in a muffle furnace that was heated and kept at 500 °C in an air ambient for 1 h.

Structural identification of the products was carried out using X-ray powder diffraction (XRD, D/max-rA) meter using Cu-Kα radiation. The morphologies of ZnO nanocrystals were observed using scanning electron microscopy (SEM, Hitachi S-4800) equipped with an energy dispersive X-ray spectrometer (EDS). Sample for transmission electron microscopy (TEM, Philips CM200) measurement was prepared by making a clear dispersion of ZnO nanoplates on carbon coated copper grid, where these ZnO nanoplates were directly scraped from substrates. Photoluminescence (PL) measurement was conducted on a Hitachi F-4500 ultraviolet–visible spectrophotometer with a Xe lamp as the excitation light source at room temperature. The excitation wavelength was 325 nm.

3. Result and discussion

After reaction, the color of aluminum surface changed from metallic sheen to faint brightness. It looks like a very thin homogenous film coated on the surface of aluminum slice. The morphology and microstructure of the films were investigated by SEM. Fig. 1 shows the images of the film on Al substrate reacted at 150 °C, i.e. sample S3, under different magnifications. An overview SEM image of the film is presented in Fig. 1a, from which one can see a porous film deposited on the substrate. The whole surface of the substrate is covered by the porous film. A magnified image in Fig. 1b clearly indicates that the porous film is composed of a large amount of plate-like nanostructures. These nanostructures are plate morphology with their 2D planes predominantly perpendicular to the substrate. According to the carefully examination from the enlarged image in Fig. 1c, these nanoplates exhibit curved anomalous morphology with a smooth surface and approximately 50 nm in thickness. They are self-assembled to form interlaced configuration and free from the cracks or holes.

The phase composition of as-obtained samples was examined by XRD. Fig. 1d shows the XRD pattern of as-deposited ZnO nanoplates on Al substrate (S3). It can be seen that the film deposited on Al substrate shows three strong peaks that fit with standard powder diffraction peaks of aluminum (JCPDS card No. 85-1327), in addition to five weak diffraction peaks of wurtzite-type phase zinc oxide. No diffraction peaks for impurities are found. It is confirmed that these oriented sheet-like nanoplates are ZnO in structure.

The thickness of ZnO nanoplates can be tuned by changing the reaction temperature. As described in Section 2, sample S1, S2 and S3 are prepared at 90, 120 and 150 °C, respectively. Parts a–c in Fig. 2 all reveal the plate morphology in the product under the same magnification. Both the thickness and planar width of the nanoplates are increased with reaction temperature. As shown in the images, nanoplates in S1, S2, and S3 are about 20, 30, and 50 nm

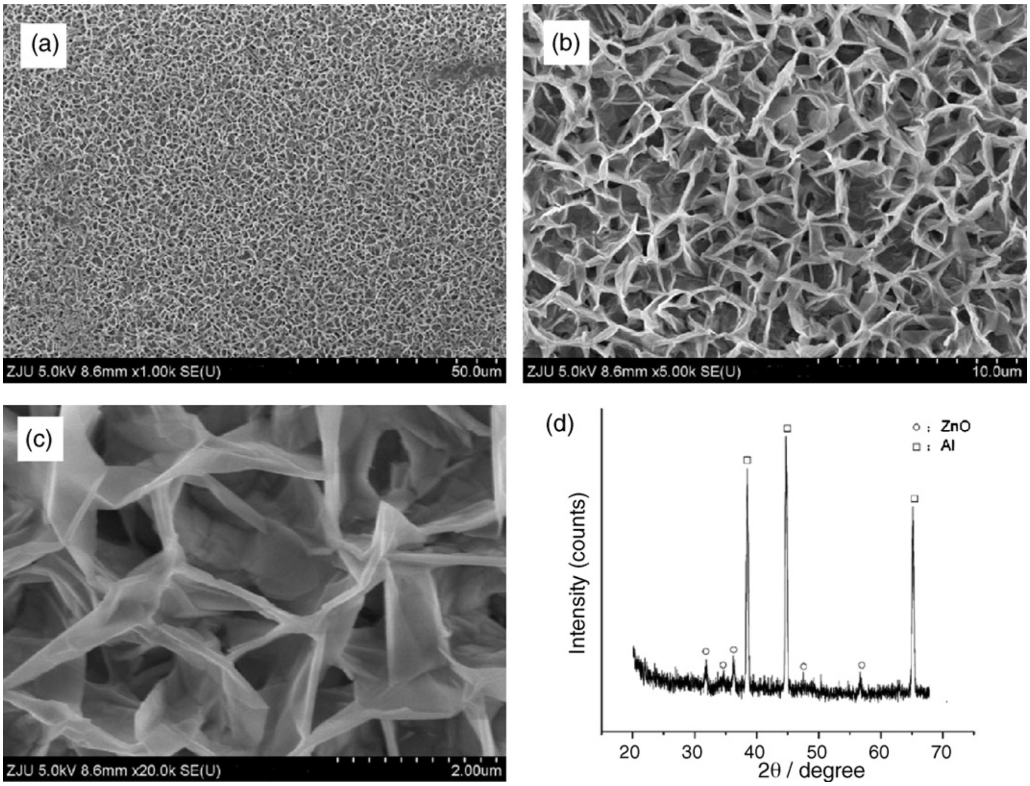

Fig. 1. SEM images of ZnO nanoplates sample S3 (a–c) and corresponding XRD pattern (d).

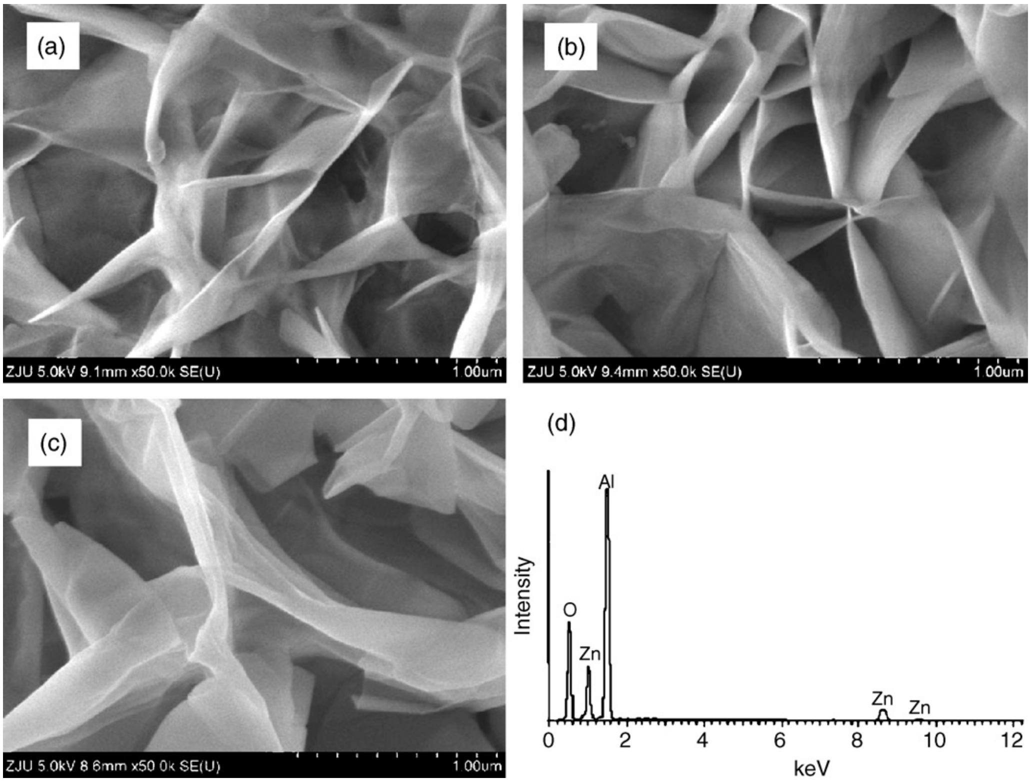

Fig. 2. SEM images of ZnO nanoplates S1 (a), S2 (b), S3 (c), and EDS pattern of S2 (d).

in thickness, respectively. These results imply that different size of ZnO nanoplates can be fabricated by controlling the reaction temperature. This is similar to what Ye reported [12], where a high pH value resulted to a thinner nanoplate. Under such a low temperature in our cases, the growth process of ZnO nanoplates cannot follow vapor–liquid–solid [18,19] and vapor–solid [4] process. The formation of ZnO nanoplates consists of three steps: formation of primary particles, coalescence of them and growth

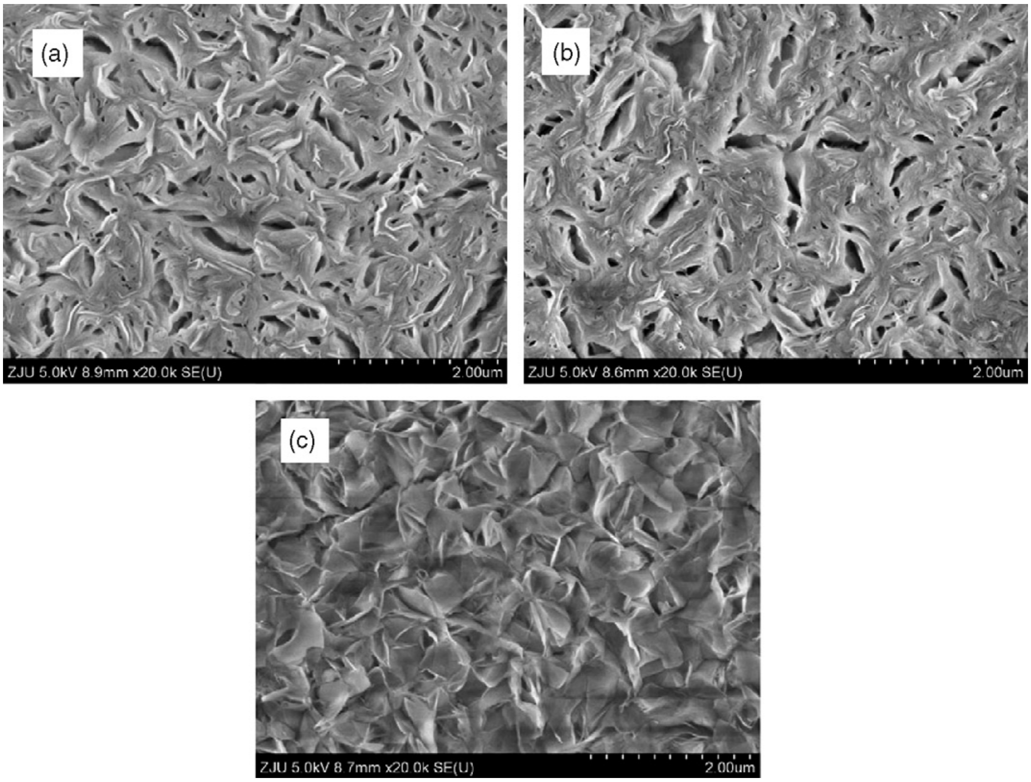

Fig. 3. SEM images of ZnO nanoplates S4 (a), S5 (b) and S6 (c).

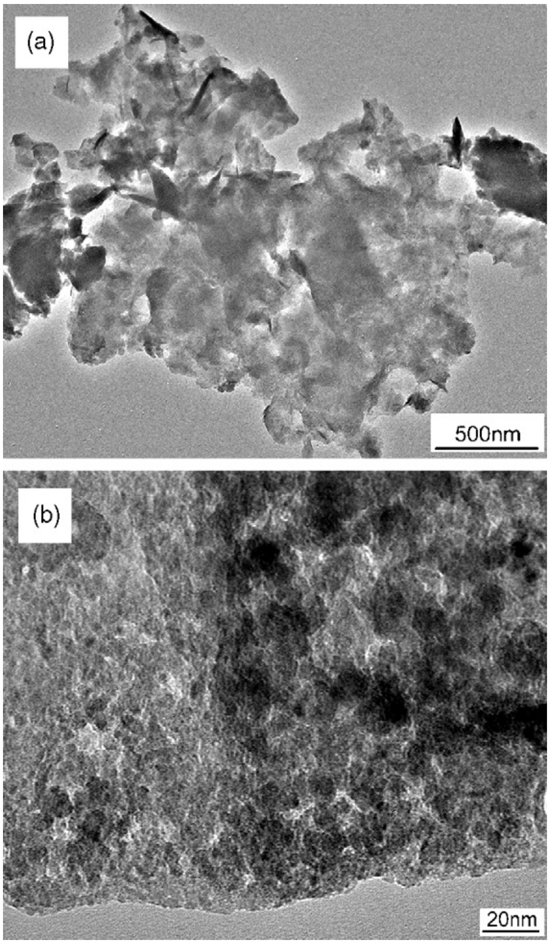

Fig. 4. (a) and (b) TEM images of ZnO nanoplate S2 under different magnifications.

of the aggregates. The size of ultimate product is related to the number of the formed aggregates under a given condition. The formation of the primary particles is fast at the initial stage at a high temperature, which is helpful to form more aggregates. In our cases, the acceleration of the primary particles should be dominant and it corresponds to the decrease of the surface free energy.

EDS was scanned for elemental analysis and to know the content of nitrogen if any in the final product as it was the part of source material. A typical EDS pattern of sample S2 in Fig. 2d shows the EDS results. The strong peaks for oxygen and zinc are noted in the spectrum. The aluminum signal results from the substrate. No other impurities such as nitrogen are detected confirming the high-purity of ZnO product. All of the ZnO samples in our experiments have a similar EDS result.

Parts Fig. 3a–c shows SEM images of S4, S5 and S6, respectively, under the same magnification. From Fig. 3a and b, one can see very dense stacked nanoplates with their lateral plane perpendicular to the substrate, when zinc concentration is 0.2 M. Tens of curved plate-like crystals are closely combined and they almost cover on all the substrate. However, the density of nanoplates is dramatically decreased, when zinc concentration is 0.02 M, as shown in Fig. 3c. It is reasonable to understand that the density of resulting ZnO nanoplates is strongly related to zinc concentration. The higher concentration of zinc is, the higher density of ZnO nanoplate is. This is a simple strategy to control the density of ZnO nanoplate on Al substrate.

TEM measurement is crucial for investigating the structure of nanocrystals as it allows a direct evolution of both the size and shape of the nanocrystals. Fig. 4 shows TEM images of ZnO nanoplates of sample S2. The image of the product accords well with the SEM results, exhibiting crooked anomalous nanoplate morphology. Sharp edges are observed. From the image contrast in Fig. 4a, it can be concluded that these ZnO nanoplates are homogeneous in thickness. The selected area electron diffraction (SAED) pattern shows diffused rings and regular spots as our previous report [17], confirming the nanocrystalline nature of ZnO nanoplates. The top and bottom wide surfaces of the nanoplates are ZnO (0 0 1) facets. However, these ZnO nanoplates could be easily destroyed and become polycrystalline ZnO under electron beam irradiation, proving these ZnO nanoplates were metastable [17]. Fig. 4b depicts a higher magnification TEM image of a nanoplate after irradiation, where it can be found that the nanoplate is made up of polycrystal grains with extremely small size, i.e. about 5 nm. These grains are single crystalline in nature (see supplementary data A).

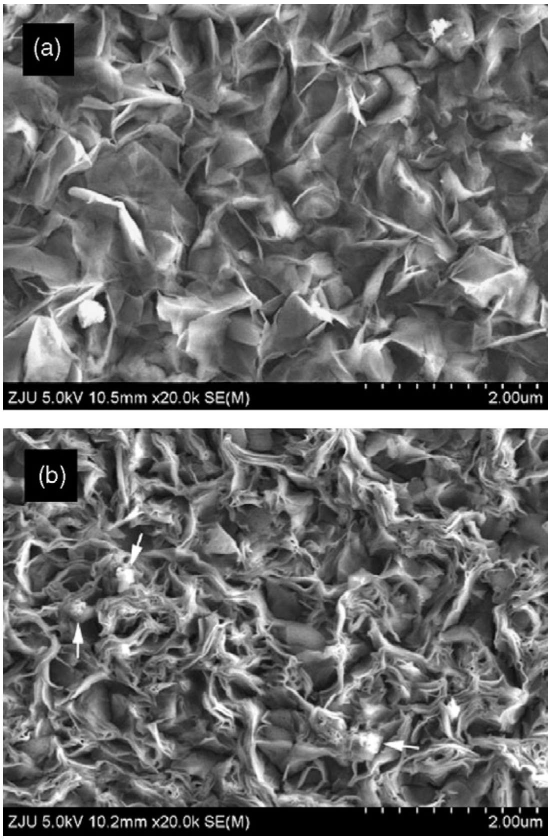

Fig. 5. SEM images of ZnO nanoplates S7 (a) and S8 (b) calcined at 500 °C.

Parts Fig. 5a and b shows the SEM morphology of samples S7 and S8, respectively. From Fig. 5a, it is found that the density of ZnO nanoplate is sparse. However, some nanoparticles are generated in the matrix of nanoplates, and it is presumed that they are ZnO crystals. Comparing sample S6 with S7, the latter is calcined from the former at 500 °C for 1 h. These ZnO nanoparticles may be caused by the recrystallization of pre-formed ZnO nanoplates. Similarly, the density of ZnO nanoplates is remarkably decreased after calcination from Figs. 3a and 5b. One can find some recrystallized ZnO nanoparticles distributed on nanoplates that are typically indicated by arrows in Fig. 5b. It is thus acceptable that the decreased density of ZnO nanoplates is caused by the recrystallization under high temperature. Moreover, the decrease in the density of ZnO nanoplate may be also attributed to the release of residual strain in the ZnO nanoplate matrix after calcination. All these provide clear-cut evidence that the solution-grown ZnO nanoplates are metastable under elevated temperature, consistent with TEM observation.

Due to its unconventional properties, the fabrication of 2D ZnO nanoplates has been intensively studied and some routes based on solution method have been developed [20–22]. However, most of 2D ZnO nanocrystals were powdered product in the case of solution method [11,20–22]. Only a few routes were devised to produce 2D ZnO nanoplates generally vertical to substrates [7–9,13,16,17], which was more convenient for nanodevices fabrication. It is well known that the fastest growth rate of ZnO is along [0 0 1] direction due to the higher surface energy under thermodynamic equilibrium conditions. Concerning 2D ZnO growth mechanism, there has a popular viewpoint in literatures that the (0 0 1) polar surface is compensated on charges by passivating agents [11,20,21]. One case was the assistance of citric acid which absorbed preferably on the (0 0 1) surface of ZnO and then slowed down the *c*-axis growth [20]. The increased concentration of OH^- in solution would prevent the new $Zn(OH)_4{}^{2-}$ ions from incorporating effectively and suppress the crystal growth along [0 0 1] direction [11]. The addition of diblock copolymers into aqueous solution could lead to a lowering of surface energy and inhibition of the growth along instinctive direction [21]. In the present case, the passivating agent to control 2D ZnO growth should be $Al(OH)_4{}^-$ [12,17] that is formed by the reaction between OH^- and Al substrate, and it is presumably attached to Zn^{2+} terminated (0 0 1) surface. The composition of ZnO nanoplates in our case actually contained aluminum measured by EDS system attached to a transmission electron microscope that allowed chemical composition to be determined at nanometer resolution [17].

Room-temperature PL measurements were performed to investigate the influence of growth and annealing temperature on the optical properties of ZnO thin film. As we known, the optical properties of semiconductors are mainly determined by the crystal quality and impurities, which are all related to the preparation conditions. But the PL spectra of S1, S2 and S3 show similar emission spectra (see supplementary data B). This may result from their low growth temperature. Fig. 6a shows the PL spectra of ZnO nanoplate films deposited on Al substrate before (sample S6) and after annealing (sample S7), respectively. For S6, it consists of a UV emission band located at about 390 nm and two blue emission bands centered at about 450 and 470 nm, respectively. The near UV emission is attributed to free-exciton recombination [23]. The blue luminescence is induced by zinc vacancies and zinc interstitial defects [24]. Concerning sample S7, there have a UV emission located at ~390 nm, a blue emission at ~430 nm and a green peak at ~505 nm. It is generally accepted that the green emission (505 nm) is related to a deep-level or trap-state emission. Vaneusden et al. [25] proved that the green transition had been attributed to the singly ionized oxygen vacancy in the ZnO. In spite of numerous studies on the visible luminescence of ZnO, its origin is still controversial [23–25]. All these blue and green emissions are related with oxygen vacancy which had an increasing trend after annealing in present case. This may result from the strong combination between Al and O and a loss of oxygen from ZnO at a higher temperature [26]. To improve the crystalline quality and the stoichiometric proportion of ZnO nanoplates, an oxygen-enriched environmental and moderate temperature are both necessary. It is clear that the emission characteristics of S8 in Fig. 6b are similar to those of S7 in Fig. 6a. The PL intensity changes of sample S8 is more remarkable than S7 after annealing, for its density of ZnO nanoplates is higher.

4. Conclusions

A large amount of ZnO nanoplates could be grown on a large scale by a simple hydrothermal process in a surfactant-free system under low temperature. These network-like nanoplates dispersed quasi-vertically and homogenously on aluminum substrates. The thickness of nanoplates was ten of nanometer. The width and thickness of the nanoplates would differ by varying the growth temperature. Increasing the temperature would result in much thicker and wider nanoplate. The density of ZnO nanoplates was strongly related to zinc concentration. After high temperature calcination, these nanoplates tended to recrystallization and its density would be decreased. The simple synthesis approach casts new light on the development of novel nanostructures for practical applications, such as nanodevices fabrication and photocatalytic degradation.

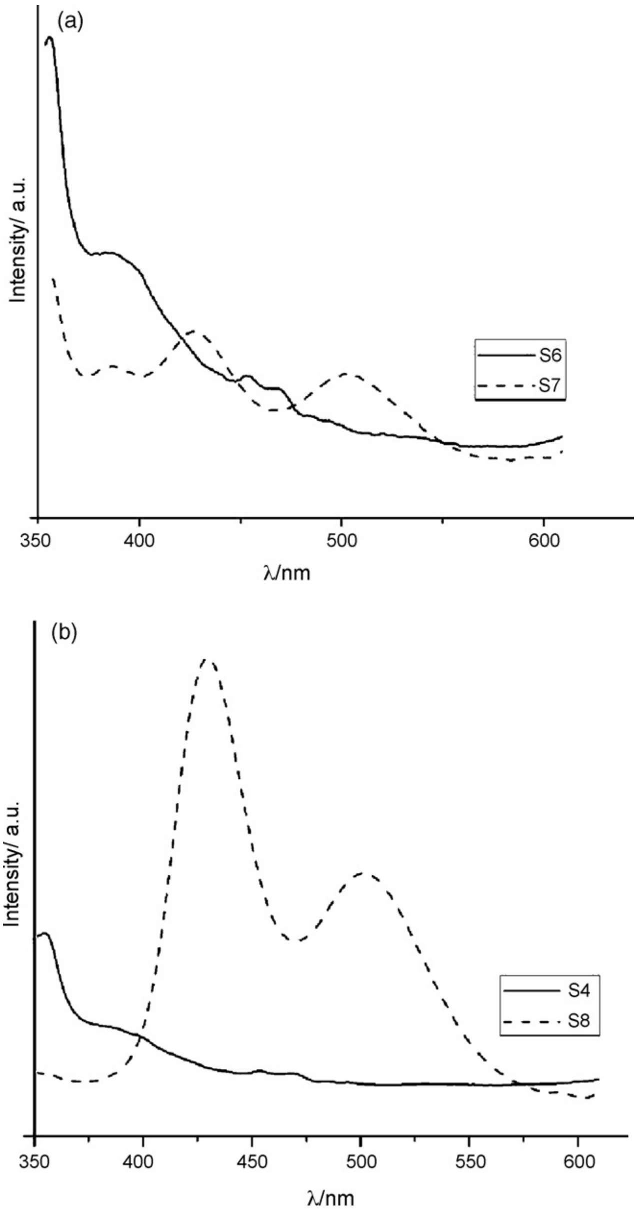

Fig. 6. PL spectra of ZnO nanoplates before and after anneal S6 and S7 (a), S4 and S8 (b).

Acknowledgments

The authors gratefully acknowledge the financial support from National Natural Science Foundation of China (No. 50571087) and Natural Science Foundation of Zhejiang Province (No. Y4080129).

Appendix A. Supplementary data

Supplementary data associated with this article can be found, in the online version, at doi:10.1016/j.jallcom.2009.02.041.

References

[1] S. Fan, M.G. Chapline, N.R. Franklin, T.W. Tombler, A.M. Cassell, H. Dai, Science 283 (1999) 512.

[2] M.H. Huang, S. Mao, H. Feick, H.Q. Yan, Y.Y. Wu, H. Kind, E. Weber, R. Russo, P.D. Yang, Science 292 (2001) 1897.

[3] J.P. Cheng, X.B. Zhang, F. Liu, J.P. Tu, H.M. Lu, Y.L. Sun, F. Chen, Mater. Chem. Phys. 87 (2004) 241.

[4] Z.Z. Ye, F. Yang, Y.F. Lu, M.J. Zhi, H.P. Tang, L.P. Zhu, Solid State Commun. 142 (2007) 425.

[5] Z.L. Wang, J. Phys. Condens. Mater. 16 (2004) R829.

[6] J.P. Cheng, X.B. Zhang, Z.Q. Luo, Physica E 31 (2006) 235.

[7] D. Paradhn, M. Kumar, Y. Ando, K.T. Leung, Nanotechnology 19 (2008) 035603.

[8] W. Bai, X. Zhu, Z.Q. Zhu, J.H. Chu, Appl. Surf. Sci. 54 (2008) 6483.

[9] K.C. Chin, C.K. Poh, G.L. Chong, J.Y. Lin, C.H. Sou, A.T.S. Wee, Appl. Phys. A 90 (2008) 623.

[10] M. Ma, J.P. Tu, Y.F. Yuan, X.L. Wang, K.F. Li, F. Mao, Z.Y. Zeng, J. Power Source 179 (2008) 395.

[11] B.Q. Cao, W.P. Cai, J. Phys. Chem. C 112 (2008) 680.

[12] C.H. Ye, Y. Bando, G.Z. Shen, D. Golberg, J. Phys. Chem. B 110 (2006) 15146.

[13] B. Illy, B.A. Shollock, J.L. Manus-Driscoll, M.P. Ryan, Nanotechnology 16 (2005) 320.

[14] E. Hosono, S. Fujihara, T. Kimura, J. Mater. Chem. 14 (2004) 881.

[15] F. Xu, Z.Y. Yuan, G.H. Du, M. Halasa, B.L. Su, Appl. Phys. A 86 (2007) 181.

[16] H.K. Sun, M. Luo, W.J. Weng, K. Cheng, P.Y. Du, G. Shen, G.R. Han, Nanotechnology 19 (2008) 125603.

[17] J.P. Cheng, X.B. Zhang, Z.Q. Luo, Surf. Coat. Technol. 202 (2008) 4681.

[18] J.P. Cheng, X.B. Zhang, Z.Q. Luo, F. Liu, Y. Ye, W.Z. Yin, W. Liu, Y.X. Han, Mater. Chem. Phys. 95 (2006) 5.

[19] J.P. Cheng, X.B. Zhang, J.P. Tu, X.Y. Tao, Y. Ye, F. Liu, Mater. Chem. Phys. 95 (2006) 12.

[20] Z.R. Tian, J.A. Voigt, J. Liu, B. Mckenzie, M.J. Mcdermott, M.A. Rodriguez, H. Konishi, H.F. Xu, Nat. Mater. 2 (2003) 821.

[21] Y. Peng, A.W. Xu, B. Deng, M. Antonietti, H. Colfen, J. Phys. Chem. B 110 (2006) 2988.

[22] Q. Xiao, S.P. Huang, J. Zhang, C. Xiao, X.K. Tan, J. Alloy Comp. 459 (2008) L18.

[23] J.P. Cheng, X.B. Zhang, X.Y. Tao, H.M. Lu, F. Liu, J. Phys. Chem. B 110 (2006) 10348.

[24] B. Liu, Z. Fu, Y.B. Jin, Appl. Phys. Lett. 79 (2001) 945.

[25] K. Vanheusden, W.L. Warren, C.H. Ceager, D.R. Tallant, J.A. Voigt, J. Appl. Phys. 79 (1996) 7983.

[26] J.G. Zhou, Y.L. Wang, F.Y. Zhao, Y.L. Wang, Y. Zhang, L. Yang, J. Lumin. 119–120 (2006) 248.